NeuroImage 150 (2017) 250–261

Contents lists available at ScienceDirect

NeuroImage

journal homepage: www.elsevier.com/locate/neuroimage

Mapping visual dominance in human sleep

Mark McAvoy[a,*], Anish Mitra[a], Enzo Tagliazucchi[b,c], Helmut Laufs[c,d], Marcus E. Raichle[a,e,f,g]

[a] Department of Radiology, Washington University, Saint Louis, MO 63110, USA
[b] Institute for Medical Psychology, Christian-Albrechts-Universitat zu Kiel, Kiel, Germany
[c] Department of Neurology, Brain Imaging Center, Goethe-Universitat Frankfurt am Main, Frankfurt, Germany
[d] Department of Neurology, Christain-Albrechts-Universitat zu Kiel, Kiel, Germany
[e] Department of Neurology, Washington University, Saint Louis, MO 63110, USA
[f] Department of Neuroscience, Washington University, Saint Louis, MO 63110, USA
[g] Department of Biomedical Engineering, Washington University, Saint Louis, MO 63110, USA

ARTICLE INFO

Keywords:
Global signal
Sleep
Hemispheric asymmetry
Lateralization
Visual network
Language network

ABSTRACT

Sleep is a universal behavior, essential for humans and animals alike to survive. Its importance to a person's physical and mental health cannot be overstated. Although lateralization of function is well established in the lesion, split-brain and task based neuroimaging literature, and more recently in functional imaging studies of spontaneous fluctuations of the fMRI BOLD signal during wakeful rest, it is unknown if these asymmetries are present during sleep. We investigated hemispheric asymmetries in the global brain signal during non-REM sleep. Here we show that increasing sleep depth is accompanied by an increasing rightward asymmetry of regions in visual cortex including primary bilaterally and in the right hemisphere along the lingual gyrus and middle temporal cortex. In addition, left hemisphere language regions largely maintained their leftward asymmetry during sleep. Right hemisphere attention related regions expressed a more complicated relation with some regions maintaining a rightward asymmetry while this was lost in others. These results suggest that asymmetries in the human brain are state dependent.

Introduction

Functional lateralization is a fundamental feature of the human brain (Gazzaniga et al., 1962). The left hemisphere's specialization for language processing was first suggested by early postmortem lesion studies (Broca, 1861; Wernicke, 1874) and has since been well documented by lesion (Damasio et al., 2004), split-brain (Gazzaniga, 1983) and task-state functional imaging studies (Price, 2012). Likewise, support for the right hemisphere's specialization for attentional processing comes from lesion (Heilman and Abell, 1980), split-brain (LeDoux et al., 1977) and task-state functional imaging studies (Cai et al., 2013). More recently, resting-state functional imaging studies have corroborated this view of functional lateralization by examining hemispheric asymmetries of the BOLD signal (Gee et al., 2011; Liu et al., 2009; McAvoy et al., 2015; Wang et al., 2013).

Functional neuroimaging of non-REM sleep has reported a variety of changes in spontaneous BOLD fluctuations. These include changes in the amplitude (Fukunaga et al., 2006), structure of temporal dynamics particularly within sensory cortices (Davis et al., 2016; Mitra et al., 2015; Tagliazucchi et al., 2013b) and in the functional connectivity within and between networks and systems (Chow et al., 2013; Spoormaker et al., 2010; Tagliazucchi et al., 2015). Thus despite global and regional reductions in cerebral blood flow, oxygen and glucose metabolism (Boyle et al., 1994; Braun et al., 1997; Buchsbaum et al., 1989; Kajimura et al., 1999; Madsen et al., 1991; Maquet et al., 1997; Nofzinger et al., 2002), non-REM sleep is not a period of quiescence (Dang-Vu et al., 2008), but rather a state of decreased interaction with the external environment and a systematic reorganization of neuronal activity (Kaufmann et al., 2006; Laufs et al., 2007). This is supported by regional increases in cerebral blood flow (Born et al., 2002; Braun et al., 1997; Kjaer et al., 2002) and BOLD signal fluctuations (Horovitz et al., 2008), after accounting for global signal changes, in the occipital lobe during light sleep compared to wakefulness. Although global BOLD signal modulations have not been explored during sleep, changes in global signal amplitude have been found to correlate with state changes resulting from sleep deprivation (Yeo et al., 2015) and electroencephalographic measures of vigilance (Wong et al., 2013).

Lateralization of function is postulated to serve the awake, alert individual who is interacting with the environment (Levy, 1969). But

* Correspondence to: Mark McAvoy, Washington University School of Medicine, 4525 Scott Ave., East Bldg, Rm 2110, Campus Box, 8225, Saint Louis, MO 63110, USA.
E-mail addresses: mcavoy@npg.wustl.edu (M. McAvoy), anishmtira@wustl.edu (A. Mitra), tagliazucchi.enzo@googlemail.com (E. Tagliazucchi), helmut@laufs.com (H. Laufs), marc@npg.wustl.edu (M.E. Raichle).

http://dx.doi.org/10.1016/j.neuroimage.2017.02.053
Received 23 December 2016; Accepted 19 February 2017
Available online 21 February 2017

what of an individual who is asleep with little interaction with the environment? Does the human brain maintain the same lateralized organization as observed during wakeful rest? Is there a functional lateralization that serves sleep? We explored hemispheric asymmetries of the global signal during wakefulness, N1, N2 and N3 sleep. Building on previous work that introduced a partial correlation model with a simple subtraction for the estimation and removal of signals common to both hemispheres (McAvoy et al., 2015), we extended this novel methodology to non-REM sleep. Although asymmetry has typically been examined by comparison of homologous regions after global signal regression (Gee et al., 2011; Liu et al., 2009; Wang et al., 2014), mapping hemispheric differences of the global signal itself has recently been validated as an effective means to quantify asymmetry (McAvoy et al., 2015). We identify a number of regions bilaterally in the visual cortex that become increasingly rightward asymmetric from the wakefulness to slow wave sleep. We show that left hemisphere language regions maintain their leftward asymmetry. Right hemisphere attention related regions show a more complicated relation with some maintaining a rightward asymmetry while this is lost in others. These changes in global signal asymmetry could not be wholly explained by regional variations in the amplitude of the spontaneous fluctuations. Since sleep is known to elicit changes in functional connectivity (Boly et al., 2012; Horovitz et al., 2009; Uehara et al., 2013), in the second part we explore the functional connectivity of left primary visual cortex with language, attention related and sensory regions.

Material and methods

Subjects, EEG-fMRI acquisition and artifact correction

Written informed consent was obtained from all subjects, and data collection was approved by the Goethe University ethics committee. Seventy-one right-handed (mean ± SD age 24.3 ± 4.7 years, range 19-48, 44 female) non-sleep-deprived subjects were scanned in the evening at ~8:00 PM. Subjects were instructed to close their eyes and lie still and relaxed. No specific instruction was given to fall asleep or maintain wakefulness. Acquisition parameters and details for these data have been previously published (Tagliazucchi et al., 2012). Briefly, fMRI was acquired in a single 52.2 min scan using a 3 T Siemens Trio (Erlangen, Germany) (1505 volumes of T2*-weighted echo planar images, TR/TE=2.080 ms/30 ms, matrix 64×64, voxel size 3×3×2 mm^3, distance factor 50%; FOV 192 mm^2) with an optimized polysomnographic setting (chin and tibial EMG, ECG, EOG recorded bipolarly - sampling rate 5 kHz, low pass filter 1 kHz) simultaneously with 30 EEG channels recorded via a cap (modified BrainCapMR, Easycap, Herrsching, Germany) with FCz as the reference (sampling rate 5 kHz, low pass filter 250 Hz, high pass filter 0.016 Hz) using MR compatible amplifiers (BrainAmp MR+, BrainAmp ExG; Brain Products, Gilching, Germany), pulse oximetry and respiration recorded via sensors from the Trio (sampling rate 50 Hz). The threshold for electrode impedances was 35 kOhm, though impedances typically remained below 30 kOhm. MRI and pulse artifact correction were performed based on the average artifact subtraction method (Allen et al., 1998) as implemented in Vision Analyzer2 (Brain Products, Germany) followed by ICA-based rejection of residual artifact components (Cardioballistogram Correction parameters; Vision Analyzer). Sleep stages were scored in 30s epochs by an expert according to the American Academy of Sleep Medicine criteria (Silber et al., 2007).

Image preprocessing

Image preprocessing included the following steps: 1) compensation for slice-dependent time shifts, 2) elimination of odd/even slice intensity differences due to interleaved acquisition (see Appendix A) and 3) realignment of all data acquired in each subject within and across runs to compensate for rigid body motion (Ojemann et al., 1997). The functional data were transformed into atlas space (Talairach and Tournoux, 1988) by computing a sequence of affine transformations (first frame of BOLD run to MP-RAGE to atlas representative target without compensation for local distortions between echo planar images and anatomy) which were combined by matrix multiplication, resampling to a 2 mm isotropic grid. For cross-modal (i.e. functional to structural) image registration, a locally developed algorithm was used (Rowland et al., 2005).

Hemispheric asymmetries

Modeling hemispheric asymmetries

Lateralized differences were examined with a hemispheric model (McAvoy et al., 2015) that included terms for the global signal (*global*), white matter (*WM*) and ventricles (*CSF*) that were separated by hemisphere (*L, R*), sleep stage (*W*, *N1*, *N2*, *N3*) and whether the scored epoch was less than 60s (*short*, *long)*. The global signal was extracted from a whole brain mask that included the cerebellum, white matter and ventricles but not extra-axial CSF, while white matter and ventricular regressors were formed from each individual's eroded white matter and ventricular masks (Power et al., 2014). Regressors were formed by removing the linear trend and intercept at each voxel, averaging over voxels in the respective hemisphere, separating into scored epochs then assigning to the appropriate *short* regressor if the epoch was less than 60s or *long* if otherwise. Although the general linear model included regressors for all sleep stages, during a given epoch as determined by the scoring, only a single regressor had values representing the BOLD fluctuations of that region (i.e. *global*, *WM* and *CSF*) while the others were set to zero. For example, during an epoch scored as 'wakefulness', the *global*, *WM* and *CSF* 'wakefulness' regressors held nonzero values, while the *N1*, *N2* and *N3* sleep regressors held zeros. Thus the regressors for the different stages were orthogonal.

Subject specific general linear models (Friston et al., 1995) were fit to BOLD time series at each voxel as shown schematically below,

$$\begin{aligned} BOLD \;=\; & global\,(L,\,R;\,W,\,N1,N2,N3;\,short,\,long)+WM \\ & (L,\,R;\,W,\,N1,N2,N3;\,short,\,long)+CSF \\ & (L,\,R;\,W,\,N1,N2,N3;\,short,\,long)+motion+lpf+c_0+c_1 t \end{aligned} \quad (1)$$

where the notation $(L, R;W, N1, N2, N3;short, long)$ represents 16 terms. Head movement signals were accounted for by *motion* which represents 24 time series formed from measured head shifts and angular displacements in three dimensions (i.e. X, Y, Z, pitch, yaw and roll) along with their squares, derivatives and squared derivatives (Friston et al., 1996). The low pass filter *lpf* was implemented with a Fourier basis set that consisted of sine and cosine pairs modeling full cycles from the cutoff of 0.08 Hz to the Nyquist frequency (Biswal et al., 1995; Lowe et al., 1998). Additional terms included the constant c_0 and linear trend $c_1 t$ to model slow drifts. The partial correlation model of Eq. 1 was solved via ordinary least squares yielding estimated weights for all regressors. Hemispheric asymmetries were explored for the *global*, *WM* and *CSF* weights for only the *long* epochs as sufficient *short* epochs were not present for further analysis (see Appendix B). Weights were normalized by the constant c_0, then spatially smoothed with a 4 mm full width at half maximum three-dimensional gaussian kernel to blur individual differences in brain anatomy.

Lateralization of the global signal: visual comparisons

Hemispheric differences of the global signal was explored visually via four independent T tests. For each stage, a subject was included in the group-level analysis if the total time summed over all *long* epochs was at least 5 min yielding 65 subjects for wakefulness, 45 subjects for N1, 35 subjects for N2 and 16 subjects for N3 sleep. Statistical significance was assessed with two-tailed, paired Student's T Tests on the difference between left and right hemisphere weights. Thus as per

Eq. 1 the four T Tests examined the following contrasts: $global(L;W;long)-global(R;W;long)$, $global(L;N1;long)-global(R;N1;long)$, $global(L;N2;long)-global(R;N2;long)$ and $global(L;N3;long)-global(R;N3;long)$. Statistical maps were z-transformed and corrected for multiple comparisons (|z|≥3.0, minimum 21 face connected voxels, $p < 0.05$ corrected) with a Monte Carlo based method (Forman et al., 1995; McAvoy et al., 2001).

Lateralization of the global signal: direct statistical comparisons

Since only ten of the 71 subjects were observed with at least 5 min of *long* epochs for each sleep stage, the direct statistical comparison of lateralization and sleep depth over all 71 subjects was one of unbalanced data that was solved with a linear mixed effects model (Bates et al., 2015). The random factor was subjects at 71 levels with fixed factors of hemisphere (*L*, *R*) and stage (*W*, *N1*, *N2*, *N3*). This analysis produced F statistics for the interaction of hemisphere by stage, the main effect of stage and the main effect of hemisphere. These maps were z-transformed and corrected for multiple comparisons (|z|≥3.0, minimum 45 face connected voxels, $p < 0.05$ corrected) with a Monte Carlo based method (Forman et al., 1995; McAvoy et al., 2001).

Global signal asymmetries and the amplitude of the spontaneous BOLD fluctuations

Six regions of interest were hand drawn on the statistical map shown in Fig. 1 according to the sleep stage with the highest peak (see Table 1). These included the left primary visual cortex, the left dorsal pars opercularis and posterior superior temporal sulcus as representative language regions and the right frontal eye field, intraparietal sulcus and temporal junction as putative attention related regions. To examine the effect of sleep depth on the amplitude of the spontaneous fluctuations and its relation to global signal asymmetries, for each subject all terms in Eq. 1 except those reflecting global signal estimates were subtracted from the BOLD time series. Thus the residual time series included only estimates relating to $global(L, R;W, N1, N2, N3;long)$ which was normalized by the value of the constant term c_0 and multiplied by 100 for units of percent BOLD signal. The standard deviation was computed across TRs for each sleep stage and averaged across subjects.

Lateralization of white matter and cerebral spinal fluid signals: direct statistical comparisons

Separate linear mixed effect models were computed for the white matter and the cerebral spinal fluid weights. These analyses were analogous to those of the global signal weights. See *modeling hemispheric asymmetries* and *lateralization of the global signal: direct statistical comparisons* for details.

Functional connectivity of left primary visual cortex

In this second part, we explored the functional connectivity of the left primary visual cortex. This region was defined on the statistical map corresponding to the difference between left and right global weights during N3 sleep (see Fig. 1, row 4, column 2).

Modeling

To explore changes in the functional connectivity of left primary visual cortex with respect to sleep depth, an additional term was added to Eq. 1,

$$\begin{aligned} BOLD = {} & global(L, R; W, N1,N2,N3; short, long)+WM \\ & (L, R; W, N1,N2,N3; short, long)+CSF \\ & (L, R; W, N1,N2,N3; short, long)+motion+lpf+c_0+c_1t+LV1 \\ & d(W, N1,N2,N3; short, long) \end{aligned} \quad (2)$$

where $LV1d(W, N1, N2, N3;short, long)$ represents eight functional connectivity terms. The creation of these regressors and normalization of the estimated weights was analogous to the global signal (see *modeling hemispheric asymmetries*).

Visual comparisons

Functional connectivity of left primary visual cortex was explored visually via four independent T tests. The criteria for subject inclusion in the group-level analysis of each stage followed that of the global signal (see *lateralization of the global signal: visual comparisons*) yielding 65 subjects for wakefulness, 45 subjects for N1, 35 subjects for N2 and 16 subjects for N3 sleep. Statistical significance was assessed with group-level two-tailed, one-sample Student's T Tests. Thus as per Eq. 2 the four T Tests examined: $LV1d(W;long)$, $LV1d(N1;long)$, $LV1d(N2;long)$ and $LV1d(N3;long)$. Statistical maps were z-transformed and corrected for multiple comparisons (|z|≥3.0, minimum 21 face connected voxels, $p < 0.05$ corrected) with a Monte Carlo based method (Forman et al., 1995; McAvoy et al., 2001).

Direct statistical comparisons

Since only ten of the 71 subjects were observed with at least 5 min of long epochs for each sleep stage, the direct statistical comparison of sleep depth over all 71 subjects was one of unbalanced data that was solved with a linear mixed effects model (Bates et al., 2015). The random factor was subjects at 71 levels with a fixed factor of stage at four levels (*W*, *N1*, *N2*, *N3*). This analysis produced F statistics for the simple main effect of stage which were z-transformed and corrected for multiple comparisons (|z|≥3.0, minimum 45 face connected voxels, $p < 0.05$ corrected) with a Monte Carlo based method (Forman et al., 1995; McAvoy et al., 2001).

Regional analyses

For regional analyses of functional connectivity the dependent variable of Eq. 2, *BOLD*, rather than being the BOLD time series of an individual voxel, was the mean time series of all the voxels in a region of interest. Eight regions of interest were explored from the analysis of global signal asymmetries and sleep depth. These included the two language and three attention related regions defined previously (see *global signal asymmetries and the amplitude of the spontaneous BOLD fluctuations* and Table 1) and three additional sensory regions drawn on the peaks of the hemisphere by stage statistical map (Fig. 1, row 5): left auditory, left somatosensory and right primary visual cortex. Correlation coefficients were computed from each subject's left primary visual cortex weights: $LV1d(W;long)$, $LV1d(N1;long)$, $LV1d(N2;long)$ and $LV1d(N3;long)$ per Eq. 2 and averaged over subjects.

Results

Sleep depth and global signal asymmetries of visual cortex

Our null hypothesis was that the ongoing fluctuations of the BOLD signal do not differ between hemispheres. This null hypothesis was tested for each sleep stage at every brain voxel with a group-level two-tailed, paired Student's T test. Fig. 1 shows statistically significant differences between the estimated left and right hemisphere global weights. Regions shown in hot colors are leftward asymmetric with a left global weight that is greater than the right, while regions in cool colors are rightward asymmetric with a right global weight that is greater than the left. Each row highlights a different stage with wakefulness in the first row progressing to N3 sleep in the fourth row. Each column presents a different view of the fiducial surface with the first and second columns showing the left hemisphere lateral and medial surfaces, and the third and fourth columns showing the right hemisphere medial and lateral surfaces, respectively. Examining the second column, the left medial surface, beginning at N2 sleep and becoming more pronounced at N3 sleep is the rightward asymmetry of early visual cortex, notably V1d. Similarly in the third column, the right medial surface, a broad swath of

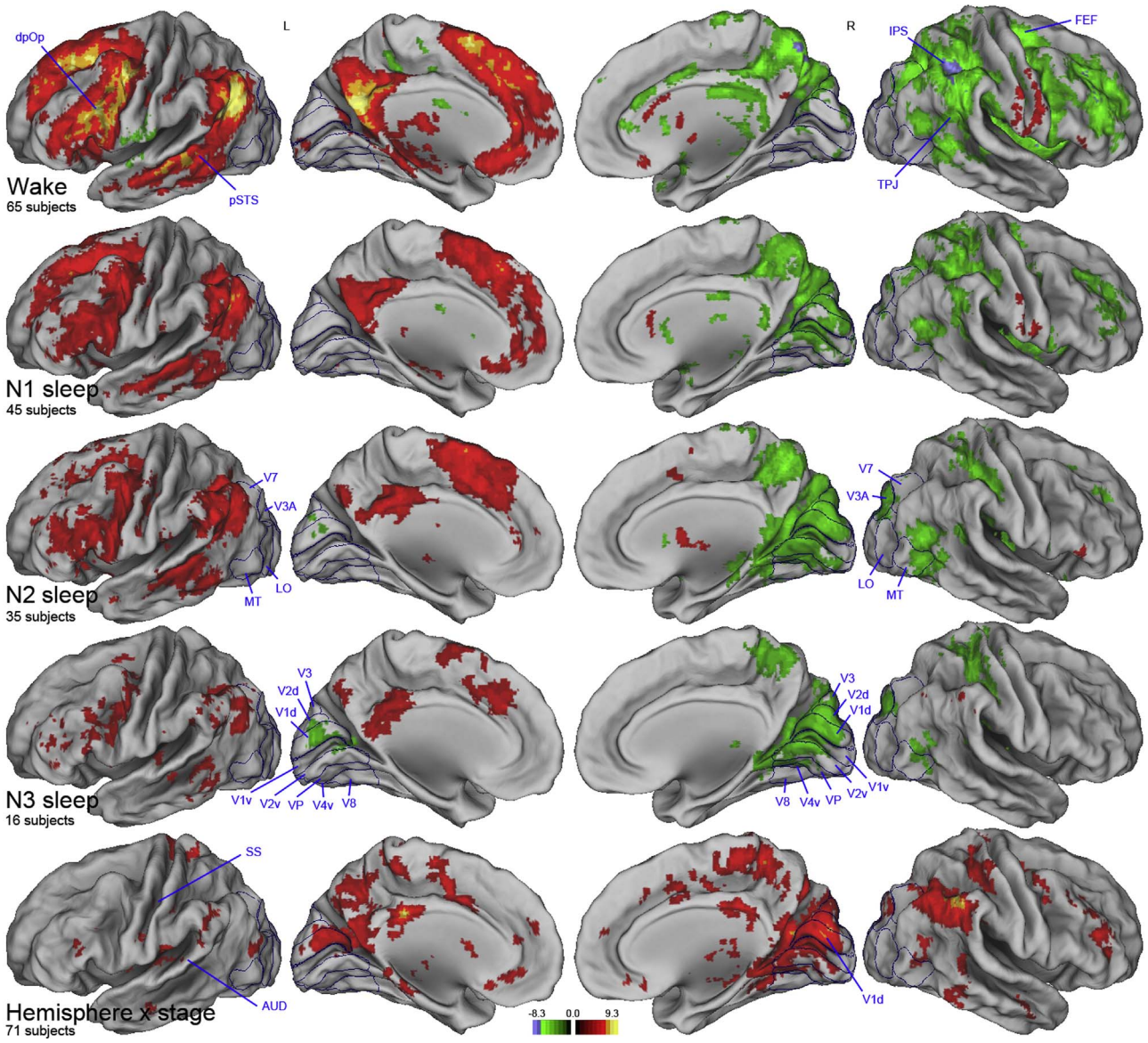

Fig. 1. Hemispheric asymmetries of the global signal. Shown in the first four rows are gaussianized T statistics from paired Student's T-tests of the difference between left and right global weights during wakefulness, N1, N2 and N3 sleep. Regions shown in hot colors display a significant leftward asymmetry. Regions shown in cool colors display a significant rightward asymmetry. Left hemisphere lateral and medial surfaces are shown in columns one and two. Right hemisphere medial and lateral surfaces are shown in columns three and four. Peak coordinates and abbreviations are listed in Table 1. On the left lateral surface, the leftward asymmetry of language regions along the inferior frontal gyrus (dpOp) and superior temporal sulcus (pSTS) are maintained from wakefulness through N2 sleep. On the medial surfaces, regions along the cuneus (e.g., V1d) and lingual gyrus (e.g., V2v) become increasingly rightward asymmetric from wakefulness through N3 sleep. On the right lateral surface, attention related regions (FEF, IPS and TPJ) show a more complicated relation. Shown in the fifth row are gaussianized F statistics of the interaction of hemisphere by stage from a linear mixed effects analysis identifying regions with significant differences between left and right global weights over the four sleep stages. Prominent on the medial surfaces is visual cortex. All maps were corrected for multiple comparisons ($P < 0.05$).

visual cortex extending from V3 to VP becomes increasing rightward asymmetric from wakefulness to N3 sleep. These observations were confirmed with direct statistical comparisons. Shown in the fifth row is the interaction of hemisphere by stage, highlighting regions with statistically significant changes in laterality with sleep depth. Prominent bilaterally on the medial surfaces is visual cortex. Thus with increasing sleep depth, regions in bilateral visual cortex become increasingly rightward lateralized. This observation is plotted for left primary visual cortex in the top row of Fig. 2. Shown is the difference between the left and right global weights averaged across subjects for each sleep stage. The increasingly downward bar with increasing sleep depth indicates increased rightward asymmetry.

Excluding TRs with a framewise displacement greater than 0.2 mm, the current recommendation for normal adult subjects (Power et al., 2014), yielded maps very similar to those of Fig. 1 (data not shown).

Sleep depth and global signal asymmetries of language and putative attention related regions

Next we examined the effect of increasing sleep depth on the asymmetry of left hemisphere language regions and right hemisphere attention related regions. In the first column of Fig. 1, the left hemisphere lateral surface, the leftward asymmetry of regions along the inferior frontal gyrus and along the posterior superior temporal sulcus is largely maintained during sleep. Direct statistical comparison suggests that lateralization of the global signal in language regions is largely unaffected by increasing sleep depth (see row 5, column 1). These observations are plotted in the top row of Fig. 2. With increasing sleep depth, a trend for decreased leftward asymmetry is found along the inferior frontal gyrus but a trend for increased asymmetry is found along the posterior superior temporal sulcus.

Table 1
Coordinates of selected regions identified in Figs. 1, 2, 4, 5 and 6.

Region	Abbreviation	Sleep stage with highest peak	Peak[c]			Volume
			x	y	z	mm^3
Left primary visual cortex[a]	LV1d	N3 sleep	1	-85	17	432
Left dorsal pars opercularis[a]	LdpOp	Wakefulness	-46	21	25	368
Left posterior superior temporal sulcus[a]	LpSTS	Wakefulness	-58	-44	1	352
Right frontal eye field[a]	RFEF	Wakefulness	21	0	60	328
Right intraparietal sulcus[a]	RIPS	Wakefulness	42	-43	43	456
Right temporoparietal junction[a]	RTPJ	Wakefulness	50	-41	15	464
Right primary visual cortex[b]	RV1d	N2 sleep	5	-81	19	400
Left auditory cortex[b]	LAUD	N3 sleep	-49	-23	12	368
Left somatosensory cortex[b]	LSS	Wakefulness	-48	-25	42	368

[a] Region was hand drawn on the statistical map of the T Test shown in Fig. 1 according to the sleep stage with the highest peak.
[b] Region was hand drawn on the statistical map of the interaction of hemisphere by stage shown in Fig. 1.
[c] Peak coordinates are given in mm according to the MNI152 atlas.

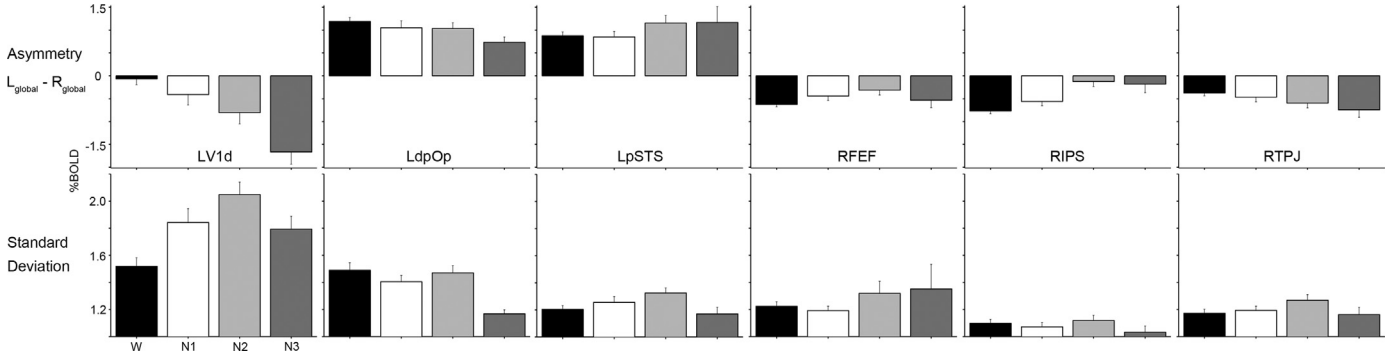

Fig. 2. Group averaged global signal asymmetries and standard deviations during wakefulness, N1, N2 and N3 sleep. Coordinates are provided in Table 1. The top row displays the difference between left and right global weights for each stage. A negative value indicates a rightward asymmetry, while a positive value indicates a leftward asymmetry. Visual cortex (LV1d) becomes increasingly rightward asymmetric from wakefulness through N3 sleep. Left hemisphere language regions along the inferior frontal gyrus (LdpOp) trend toward decreased leftward asymmetry, while regions along the posterior superior temporal sulcus (LpSTS) trend toward increased leftward asymmetry. Right hemisphere attention related regions (RFEF, RIPS and RTPJ) show a variable relation in their rightward asymmetry. The bottom row displays the amplitude of the spontaneous fluctuations. All terms in Eq. 1 except those reflecting the global signal were regressed from the BOLD time series, thus the standard deviation reflects only global signal modulations. Although there is some correspondence between changes in asymmetry and standard deviation, the relation is equivocal. For example, while the rightward asymmetry of LV1d increases from awake through N3 sleep, the standard deviation increases only through N2 sleep. Percent BOLD signal was computed for each subject by normalizing to the value of the constant term, then multiplying by 100. Displayed are the mean percentages across subjects.

Now consider the last column of Fig. 1, the right hemisphere lateral surface. Beginning in N2 sleep, rightward asymmetry is lost along much of the intraparietal sulcus and frontal eye field, while the temporoparietal junction maintains some degree of asymmetry. Direct statistical comparison (see row 5, column 4) reveals that asymmetry is modulated by sleep depth in part for all three regions. The top row of Fig. 2 indicates that with increasing sleep depth, asymmetry decreases in the frontal eye field from wakefulness through N2 sleep then increases during N3 sleep, while asymmetry deceases along the intraparietal sulcus and increases along the temporoparietal junction.

Lateralization of the global signal and the amplitude of the spontaneous BOLD fluctuations

In the top row of Fig. 2 some regions increased in asymmetry with sleep depth (primary visual cortex, the left posterior superior temporal sulcus and the right temporoparietal junction), while others decreased (left dorsal pars opercularis and the right intraparietal sulcus) and still others exhibited a variable relation (right frontal eye field). To see if changes in asymmetry were simply tracking amplitude modulations of the underlying spontaneous BOLD fluctuations, we computed the standard deviation for each sleep stage. Consider the first column of Fig. 2 which highlights asymmetries (top row) and standard deviations (bottom row) for a region in primary visual cortex. While increases in asymmetry and amplitude track each other through N2 sleep (Tagliazucchi and Laufs, 2014; Tagliazucchi et al., 2013b), the substantial increase in rightward asymmetry in N3 sleep is accompanied by a decrease in amplitude. Similar correspondences are observed for the other regions. Clearly there is some relation between asymmetry and amplitude with sleep depth, but it is equivocal.

Sleep depth and asymmetries of white matter and cerebrospinal fluid signals

It is possible the effects of global signal asymmetry and sleep depth observed in visual cortex, language and attention related regions are secondary or perhaps residual effects of larger changes in white matter and cerebrospinal fluid signals. To test this hypothesis, direct statistical comparisons via linear mixed effects were performed. Shown in Fig. 3A is the interaction of hemisphere by stage for white matter signals. Most notable are significant effects along the left medial surface (column 2) dorsally in primary visual cortex extending into the junction of the parieto-occipital and calcarine sulcus, anteriorly into the posterior cingulate gyrus and dorsally into the precuneus. Plotting the difference in white matter signals between hemispheres for primary visual cortex, asymmetries were seen to be much smaller compared to the global signal (see Fig. 2, top row). The largest difference was a leftward asymmetry observed for N3 sleep which was much smaller than the rightward asymmetry of the global signal. On the right lateral surface (Fig. 3A, column 4), significant changes were observed along the temporoparietal junction, but these white matter signals were left

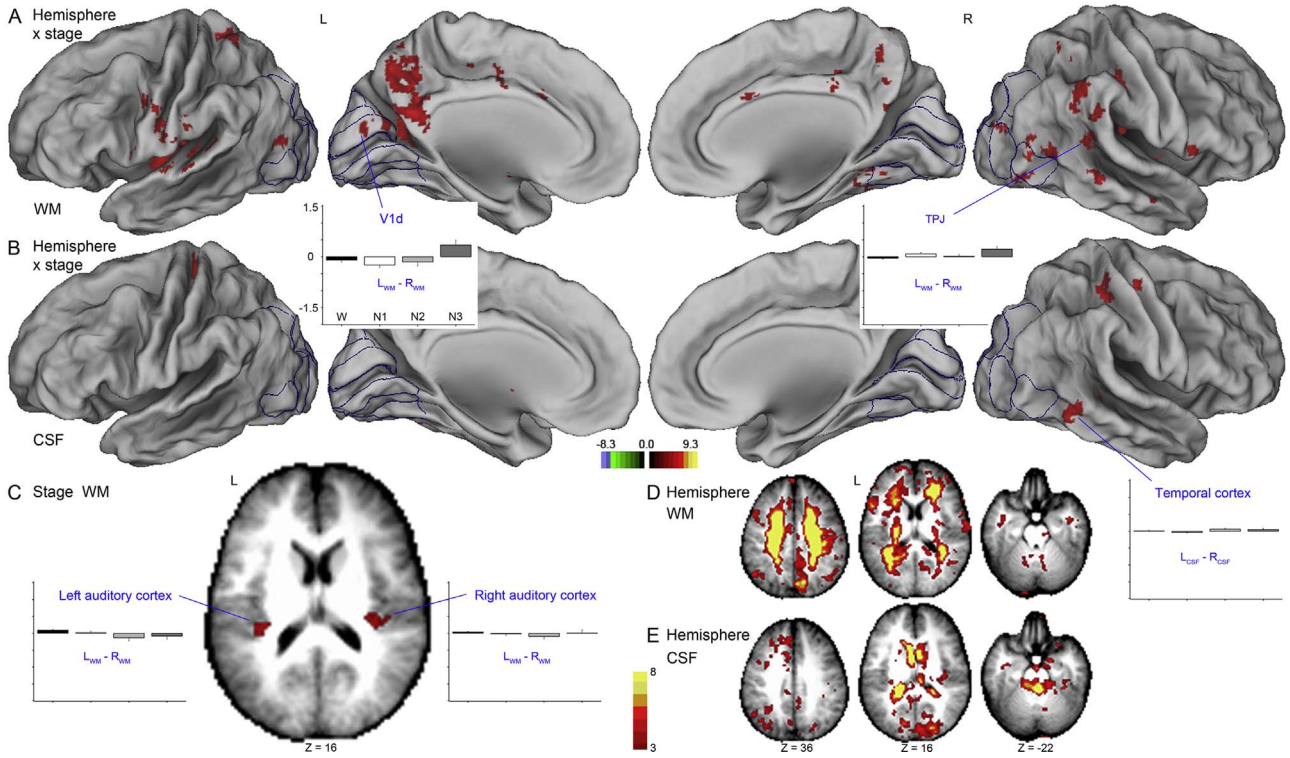

Fig. 3. Direct statistical comparisons of hemispheric asymmetries of white matter and cerebrospinal fluid signals. A. Interaction of hemisphere by stage for white matter signals. Plotted is the difference in white matter signals between hemispheres for primary visual cortex (V1d) and the temporoparietal junction (TPJ). B. Interaction of hemisphere by stage for cerebrospinal fluid signals. Plotted is the difference in cerebrospinal fluid signals for a region in temporal cortex. C. Main effect of stage for white matter signals. Highlighted in the axial slice is a bilateral region in auditory cortex with underlying white matter. D. Main effect of hemisphere for white matter signals. E. Main effect of hemisphere for cerebrospinal fluid signals. Displayed are gaussianized F statistics from linear mixed effects analyses corrected for multiple comparisons ($P < 0.05$).

lateralized in contrast to the larger right lateralized global signals (see Fig. 2, top row).

Few effects of sleep depth and asymmetry were seen for cerebrospinal fluid signals which were less prevalent and smaller than white matter signals (see Fig. 3B). The main effect of sleep depth was not significant for cerebrospinal fluid signals, but a bilateral region in auditory cortex with underlying white matter survived multiple comparisons for white matter signals. Although this region lacked significant changes in asymmetry, modulations with sleep depth were significant but rather small (see Fig. 3C).

Where is the white matter and cerebrospinal fluid? These effects were found in the main effect of hemisphere (Figs. 3D and 3E). Thus white matter and ventricular regions though they show significant asymmetries, these asymmetries were not modulated by sleep depth.

Asymmetry of primary visual cortex and functional connectivity

We were particularly interested in any observed changes in the functional connectivity of primary visual cortex and the rest of the brain, as left primary visual showed dramatic increases in rightward asymmetry with sleep depth (see Fig. 2, top row). Shown in the first row of Fig. 4 is the functional connectivity of left primary visual cortex during wakefulness, the second row during N1, the third during N2 and the fourth during N3 sleep. Displayed in the fifth row is the main effect of stage from a linear mixed effects analysis highlighting regions with statistically significant changes in functional connectivity with left primary visual cortex as a function of sleep depth.

Functional connectivity of primary visual cortex with language regions

We first examined the functional connectivity of left primary visual cortex with left hemisphere language regions along the inferior frontal gyrus and the superior temporal sulcus. Consider the axial slices displayed in the second column of Fig. 4 (Z=26). During wakefulness little connectivity is seen along the inferior frontal gyrus (dpOp, top row) in the left hemisphere in contrast to the right. However, beginning in N1 sleep increased anticorrelation is seen along the left inferior frontal gyrus. Similar observations are found for the posterior superior temporal sulcus in the fourth column (pSTS, Z=0). Direct comparison (row 5) indicated these changes were statistically significant. This increase in anticorrelation is plotted in the first two columns of Fig. 5.

Functional connectivity of primary visual cortex with attention related regions

We next examined the functional connectivity of left primary visual cortex with right hemisphere attention related regions. In the first column of Fig. 4 (Z=42), visual inspection suggests functional connectivity is maintained along the intraparietal sulcus through all sleep stages. In fact, direct statistical comparison (row 5) indicates a significant increase in anticorrelation with sleep depth (see Fig. 5). In the third column of Fig. 4 (Z=12), a sign change is observed along the temporoparietal junction with a positive correlation during wakefulness compared to the anticorrelation during sleep. This statistically significant change is plotted in Fig. 5. Connectivity with the frontal eye field is variable with changing levels of anticorrelation (see Fig. 5). In contrast to the intraparietal sulcus and temporoparietal junction, these changes were not statistically significant. Unlike left hemisphere language regions, right hemisphere attention related regions lacked an easily discernable pattern in their connectivity with primary visual cortex to changes in sleep depth.

Functional connectivity of primary visual cortex with sensory systems

Examining primary visual cortex's relationship with other sensory cortices, connectivity was lost with auditory cortex during sleep as seen

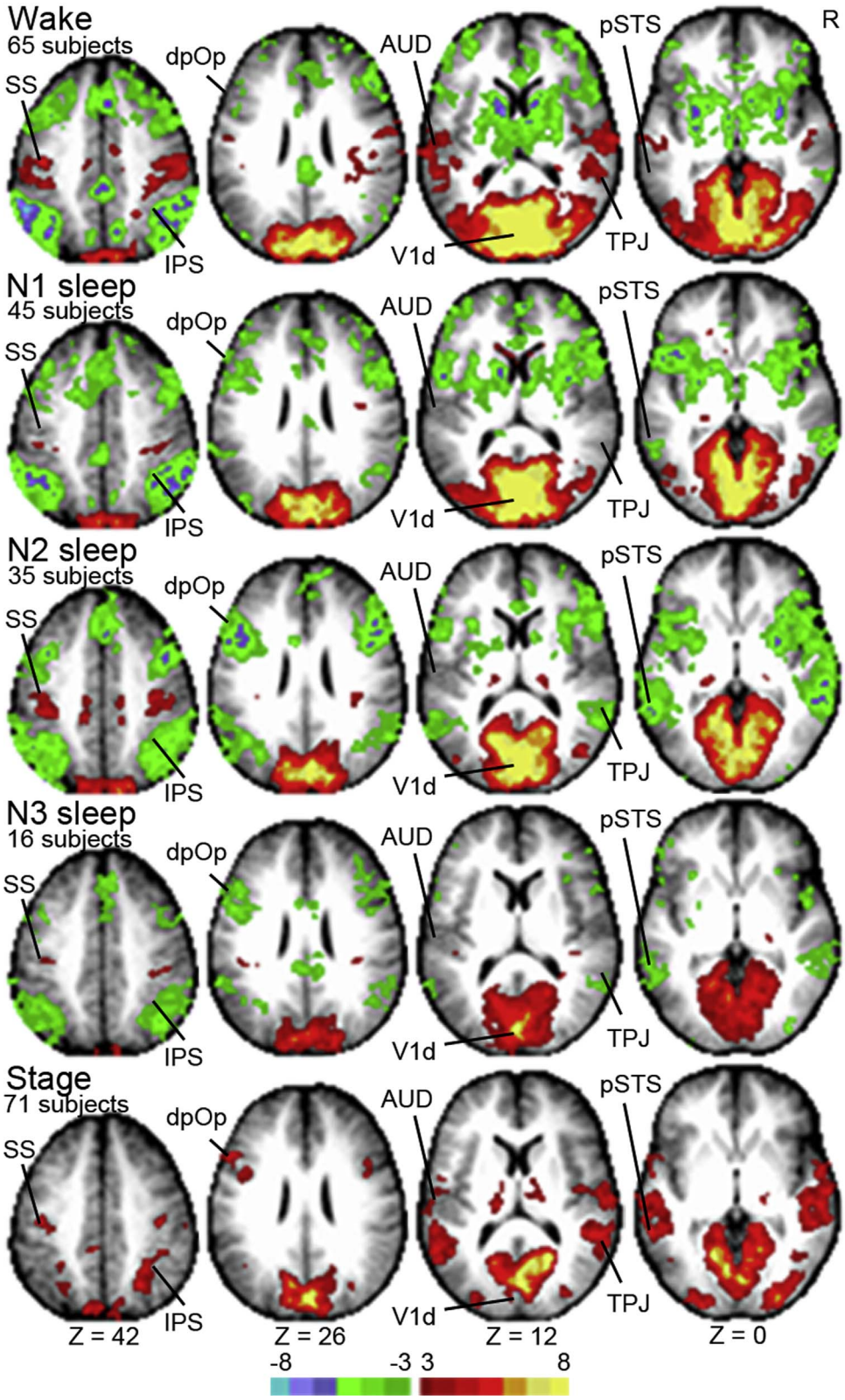

Fig. 4. Functional connectivity of left primary visual cortex. Shown in the first four rows are gaussianized T statistics from one-sample Student's T-tests during wakefulness, N1, N2 and N3 sleep. Shown in the fifth row are gaussianized F statistics of the main effect of stage from a linear mixed effects analysis highlighting regions with statistically significant changes in functional connectivity with sleep depth. Beginning in N1 sleep, the loss of connectivity with auditory cortex (AUD, column 3) is accompanied by increased anticorrelation with left hemisphere language regions (dpOp, column 2 and pSTS, column 4) and along the right intraparietal sulcus (IPS, column 1). The connectivity relation with regions in somatosensory cortex (SS, column 1) and the temporoparietal junction (TPJ, column 3) is more complex. All maps were corrected for multiple comparisons ($P < 0.05$).

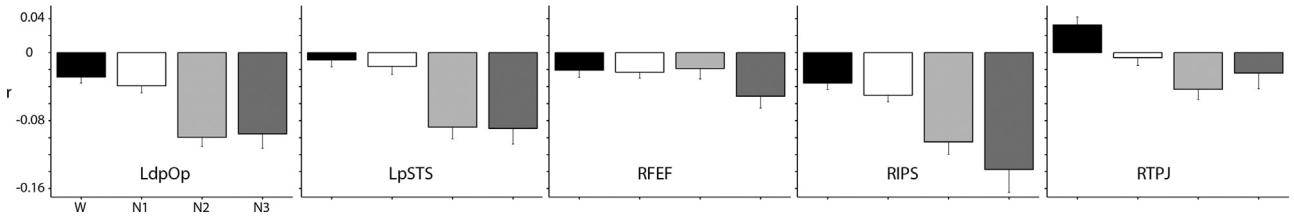

Fig. 5. Functional connectivity of left primary visual cortex with left hemisphere language regions (LdpOp and LpSTS) and right hemisphere attention related regions (RFEF, RIPS and RTPJ). Plotted are subject averaged correlation coefficients. Coordinates are provided in Table 1. While language regions show increased anticorrelation with sleep depth, attention related regions show a variable relation.

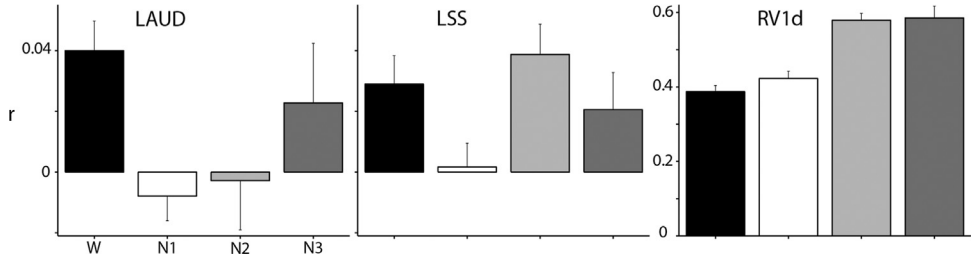

Fig. 6. Functional connectivity of left primary visual cortex with sensory systems, including auditory (LAUD), somatosensory (LSS) and visual (RV1d). Plotted are subject averaged correlation coefficients. Coordinates are provided in Table 1. A sharp reduction in correlation from wakefulness to N1 sleep is observed in left auditory (LAUD) and left somatosensory (LSS) cortex, while a positive correlation is maintained with the homotopic counterpart (RV1d).

in the third column of Fig. 4 (Z=12), while connectivity with somatosensory cortex waxed and waned (first column, Z=42). These statistically significant changes (row 5) are highlighted in Fig. 6 where a marked decrease in connectivity was observed from wakefulness to N1 sleep in both auditory and somatosensory cortex. During N2 sleep, a positive correlation was reestablished with somatosensory cortex. Curiously, during N3 sleep auditory cortex trended toward positive correlation. These changes in relation to other sensory systems occurred while left primary visual cortex maintained connectivity with its homologous counterpart.

Summary of functional connectivity

With increasing sleep depth, left primary visual cortex became increasingly anticorrelated with left hemisphere language regions and the right intraparietal sulcus. Beginning in N1 sleep, connectivity was greatly decreased with other sensory systems and the temporoparietal junction. During N2 sleep, increased connectivity was observed with the somatosensory system and along the temporoparietal junction which decreased during N3 sleep. Also during N3 sleep, a trend towards positive connectivity was found in auditory cortex. Left primary visual cortex's connectivity with the frontal eye field was not modulated by sleep depth and maintained with its homologous counterpart.

Discussion

Sleep and lateralization of function in the human brain

Lateralization of function in the awake state has been supported by lesion (Bates et al., 2001; Mapstone et al., 2003; Rabuffetti et al., 2012), split-brain (Gazzaniga, 2000) and task (Cai et al., 2013; Kristensen et al., 2013; Pardo et al., 1991; Price, 2010; Shulman et al., 2010) and resting state neuroimaging studies (McAvoy et al., 2015; Wang et al., 2014) which have advanced the left hemisphere's specialization for language processing and right hemisphere's specialization for attentional processing. Despite the inherent difficulty of getting subjects to sleep in the fMRI environment, sleep provides a means to explore state changes in absence of external stimulation (Fransson et al., 2009). Although sleep is postulated to be an actively regulated process wherein neuronal activity is reorganized (Hobson, 2005), the functional role of sleep has yet to be fully elucidated. In addition to the possibly of promoting the clearing of toxins from the brain (Xie et al., 2013), evidence suggests that there are active neural computations important for learning and memory which occur during sleep (Diekelmann and Born, 2010; Walker and Stickgold, 2006).

The underlying stages of sleep and the amount of time an individual spends in them changes throughout one's lifetime (Ohayon et al., 2004). Characterization of the intrinsic brain activity of normal, healthy individuals is currently of great importance especially with the disturbed sleep of many individuals suffering from such common diseases as Alzheimer's (Stelzmann et al., 1995), frontotemporal dementia (Anderson et al., 2009) and Parkinson's (Chaudhuri et al., 2006). Sleep and its relation to disease has garnered increased interest as a bidirectional relationship has been established in neurocognitive diseases whereby disease progression has been associated with impaired sleep; likewise impaired sleep has been found to be correlated with increased severity of disease progression (Ju et al., 2014). Notably, in addition to memory impairments (Gold and Budson, 2008) disease progression is commonly marked by language impairments (Taler and Phillips, 2008) and declines in attentional and visuospatial abilities (Weintraub et al., 2012). Perhaps a functional lateralization also serves sleep, and loss of this lateralization as observed through hemispheric asymmetries of the global signal may prove to be an effective biomarker to predict disease progression (Hahamy et al., 2014).

Rightward asymmetry of bilateral visual cortex during sleep may reflect visual processing dominance

Is there any evidence to suggest that visual processing is right lateralized? A recent functional neuroimaging study in which subjects passively viewed a full field checkerboard stimulus found larger evoked BOLD responses in the right hemisphere for regions in both early and higher-level visual cortex, with no relation to eye dominance (Hougaard et al., 2015). In the task-state, larger evoked BOLD responses to visually guided saccades were found in the right calcarine sulcus (i.e. V1v) and MT compared to their left hemisphere homologues (Petit et al., 2015). These results suggest a rightward asymmetry in the processing of visual stimuli. During slow wave sleep, a trend toward greater right hemisphere MEG slow-wave activity in early visual cortex has been measured (Tamaki et al., 2016). Consistent with this finding, we observed greater rightward global signal asymmetry to

increased sleep depth in early visual cortex (Fig. 2, top row, LV1d). Thus both the task and sleep data are in agreement with regard to the possible rightward lateralization of visual areas.

Considering Fig. 2 once again, the increasing asymmetry of visual cortex appears to be the best correlate of sleep stage. Consistent with this speculation, increased regional cerebral blood flow in medial occipital cortex has been found to correlate with increased EEG delta activity (Hofle et al., 1997), an electrophysiological marker of sleep depth. Also MEG slow-wave activity has been found to increase with increasing sleep depth in visual areas (Tamaki et al., 2014). Thus despite global reductions in metabolism (Boyle et al., 1994), non-REM sleep is a period of relatively increased neural activity in occipital cortex in which functional connectivity is reorganized (Altmann et al., 2016), while cross-hemispheric functional connections are maintained (see Fig. 6). Our results extend these observations with the increased functional connectivity of visual cortex with left lateralized language regions during sleep despite connectivity changes with other sensory systems and attention related regions (Figs. 4, 5 and 6).

Given greater rightward asymmetry from wakefulness to N3 sleep in visual cortex (Fig. 2, top row), would one expect a correspondingly greater amount of imagery in the deeper sleep stages? Such an expectation is not only at odds with published reports as slow wave sleep (i.e. N3) has the poorest recall of visual imagery (Foulkes and Scmidt, 1983) but also with subject reports from this data set which found the perception of inner speech and visual imagery correlated positively with BOLD signals only during N2 sleep when compared to wakefulness in left temporal and visual cortex, respectively (Tagliazucchi et al., 2013a). This is consistent with the decoding of self-generated visual imagery (Horikawa et al., 2013) and the greater recall of task specific stimuli after light sleep (Deuker et al., 2013). These observations lie in contrast to impaired visual perceptual learning without sufficient slow wave sleep (Walker and Stickgold, 2006). Quite speculatively, the increasing asymmetry of visual cortex with sleep depth, rather than being a metric for visual imagery, may differentiate between types of visual processing from replay in light sleep progressing to memory processes in slow wave sleep.

Relevance of global signal asymmetries

The novelty of our approach to asymmetry is that it maps differences in the global signal between hemispheres by investigating the correlation between the regional signal and the left and right-half global signal. In contrast to methods that have examined homologous regions after removing the global signal (Gee et al., 2011; Liu et al., 2009; Wang et al., 2013), hemispheric asymmetry mapping does not suffer from the difficulty in defining appropriate ipsilateral and contralateral regions for comparison. Although the global signal includes components that are non-neuronal in origin including cardiac (Shmueli et al., 2007), respiratory (Wise et al., 2004) and head movement signals (Power et al., 2012; Zeng et al., 2014), computing the difference between hemispheres removes signals common to both hemispheres supporting the notion that the global signal possesses an important neuronal component (Scholvinck et al., 2010). Further support for a neural origin comes from resting state functional connectivity analyses as global signal regression changes the topography among and relationship between systems (Weissenbacher et al., 2009). The focus of this controversy is whether the anticorrelations observed after global signal regression represent a bona fide relation relevant to brain function or are merely an induced artifact (Fox et al., 2009). This confounding factor versus nuisance variable debate seems to relegate the global signal to a secondary role far behind the so-called resting state networks. Recent work has attempted to infer sleep stage from changes in the relations within and between resting state networks (Altmann et al., 2016; Tagliazucchi et al., 2012). It is curious that something as simple as examining the hemispherical difference of the global signal in visual cortex may hold promise as a robust measure of sleep depth (see Fig. 2, top row). Perhaps within the global signal is a layer of organization on par if not primary to the brain's systems, and we've only begun to uncover it.

Conclusions and limitations

Earlier work exploring hemispherical asymmetries of the global signal in awake fixating subjects (McAvoy et al., 2015) reported a leftward asymmetry for left hemisphere regions preferential for language processing and a rightward asymmetry for right hemisphere regions related to attentional processing. In this work, we explored the effect of sleep on these asymmetries and found that while the leftward lateralization of the language network was largely maintained during sleep, the rightward lateralization of the attention network was maintained in some regions but decreased in others. Of great interest was the increased rightward asymmetry of bilateral visual cortex. These changes in global signal asymmetry could not be wholly explained by regional changes in the amplitude of the spontaneous fluctuations and were accompanied by changes in functional connectivity that were not dependent on regional asymmetry. This suggests that lateralization does not merely reflect the underlying neuroanatomical structure, rather neuromodulators play an active role (Bargmann and Marder, 2013; Tucker and Williamson, 1984).

These observations must be tempered with the fact that a smaller pool of subjects was observed for each stage of increased sleep depth. As a result, the power to detect significant differences in the global signal between hemispheres also decreased (Fig. 1), as well as the power to map the functional connectivity of primary visual cortex (Fig. 4). Thus it is important to consider the effect sizes themselves (Figs. 2, 3, 5 and 6) as results of equal significance obtained with a lesser number of subjects imply a larger effect size (Friston, 2012). It must also be stressed that this is just a first exploration that lacks the replication of an independent data set; however, getting subjects to sleep in the fMRI environment especially with the addition of the peripheral equipment necessary to record physiological signals is very challenging (Laufs et al., 2007).

Funding

This work was supported by the Mallinckrodt Institute of Radiology (MIR 12-023 and MRF 3618-92508 to M.M.), National Institutes of Health (NINDS NS080675 to M.E.R., F30MH106253 to A.M.), Bundesministerium für Bildung und Forschung (01EV0703 to H.L. and E.T.) and the LOEWE Neuronale Koordination Forschungsschwerpunkt Frankfurt (H.L. and E.T.). This study was supported in part by the Neuroimaging Informatics and Analysis Center (1P30NS098577).

Conflict of Interest

The authors report no conflict of interest.

Acknowledgements

We thank Deanna Barch, Avi Snyder, Becky Coalson, Fran Miezin and Erik Herzog for helpful discussions, and the reviewers whose constructive criticisms greatly improved this manuscript.

Appendix A

A. Correction of odd/even slice intensity differences

Assume that odd and even slices are affected by alternating multiplicative intensity errors. Thus, for every voxel in an even slice, the measured intensity is $\tilde{v}_{ik}=v_{ik}(1+\alpha)$, where v_{ik} (always positive) is the unbiased (true) intensity and the subscript indexes voxel i in slice k. Similarly, in odd slices, the measured intensity is $\tilde{v}_{ik}=v_{ik}(1-\alpha)$. Thus, measured intensities on successive slices are biased in the opposite direction. They key operational assumption is that the true intensity profile across slices is, on average, locally linear. Accordingly, the average measured intensity on the slices above and below will differ from the current slice by $2s\alpha v_{ik}$, where $s=(-1)^k$ depends on the parity of the slice index. Therefore, ignoring the difference between v_{ik} and $\tilde{v}_{ik}$, we have

$$(1/2)(\tilde{v}_{i(k+1)}+\tilde{v}_{i(k-1)})-\tilde{v}_{ik}\approx 2s\alpha\tilde{v}_{ik} \tag{A.1}$$

To solve for α, both sides of Eq. A.1 are weighted by $\tilde{v}_{ik}$, to emphasize bright voxels, and the resulting quantities are summed over the available data.

$$\alpha=\frac{\sum_{ik}[(1/2)(\tilde{v}_{i(k+1)}+\tilde{v}_{i(k-1)})-\tilde{v}_{ik}](-1)^k\tilde{v}_{ik}}{2\sum_{ik}\tilde{v}_{ik}^2} \tag{A.2}$$

Having estimated α, the measured data are corrected by inverting $\tilde{v}_{ik}=v_{ik}(1+\alpha)$.

Appendix B

B. Sleep demographics

(See Appendix Tables B1 and B2).

Table B1
Total time (min) of the sleep staged epochs for the 71 subjects.

			Long (≥ 1 min)				Short (< 1 min)							Long (≥ 1 min)				Short (< 1 min)			
	Sex	Age	W	N1	N2	N3	W	N1	N2	N3		Sex	Age	W	N1	N2	N3	W	N1	N2	N3
1	F	19	28.5	14.5	5.0		1.5	2.0	0.5		37	F	21	34.5	13.0	2.0		1.5	1.0		
2	F	21	48.3	2.0			0.5	1.2			38	M	23	21.5	9.0	14.0	3.0	0.5	2.8	1.2	
3	F	22	12.5	10.0	22.0		0.5	5.0	1.9		39	F	29	52.0							
4	F	22	40.5	10.5			1.0				40	M	23	52.0							
5	F	20	8.3	9.0	11.0	19.7		0.5	1.0	2.4	41	F	27	17.2	13.7	18.9			0.7	1.5	
6	M	25	20.3	23.2			5.4	3.1			42	M	29	52.0							
7	F	24	10.8	4.5	11.5	19.5	1.5	3.0	0.7	0.5	43	F	21	50.0	1.0				1.0		
8	F	22	44.3	7.2				0.5			44	F	24	32.5	4.0	15.0			0.5		
9	M	27	50.5					1.5			45	M	23	44.5	7.5						
10	F	20	38.9	8.5			1.5	3.1			46	M	22	2.8	48.7			0.5			
11	F	29	48.9	1.0				2.0			47	M	22	7.5	6.2	22.9	13.5	0.8	1.0		
12	M	24	49.8				1.2	1.0			48	F	23	23.8	11.5	10.5		1.7	2.9	1.5	
13	F	48	36.2	6.5			2.8	6.5			49	F	23	2.7	1.3	21.5	22.5	1.2	1.8		1.0
14	F	29	34.5	10.5			3.2	2.9	1.0		50	F	23	20.5	9.5	20.0		0.5	1.0	0.5	
15	F	29	38.5	5.0	7.5		0.5	0.5			51	M	30	10.7	10.1	20.5	4.0	0.5	1.0	3.7	1.5
16	M	31	13.2	33.0	2.0		2.3	1.0	0.5		52	M	21	19.8	7.0	15.5	6.7	0.5		1.5	1.0
17	M	36	52.0								53	F	22	48.5	1.0			0.5	1.9		
18	F	25	22.8	14.5	7.0	7.2		0.5			54	M	26	3.8	7.0	22.3	17.0	1.0		0.5	0.5
19	M	25	29.0	10.6	9.5		1.0	1.0	0.9		55	M	23	8.3	9.9	17.7	14.0		1.1	0.5	0.5
20	F	23	16.7	18.0	16.7				0.5		56	M	22	52.0							
21	M	26	25.3	20.5	2.5		1.8	1.9			57	M	24	14.5	7.5	13.0	12.5	1.6	1.9	1.0	
22	F	29	28.0	14.9	7.5		0.6	1.0			58	F	20	2.3	18.0	29.1		1.7	1.0		
23	F	23	18.5	11.0	16.6	4.2	0.5	0.2	1.0		59	F	21	50.3				0.7	1.0		
24	M	21	3.8	3.0	10.0	34.7		0.5			60	F	22	40.8	10.7			0.5			
25	F	22	27.5	5.0	14.5		2.0	2.0	1.0		61	F	21	11.5	3.5	10.0	26.5		0.5		
26	F	21	12.5	12.0	7.0	20.5					62	F	24	52.0							
27	M	40	51.0					1.0			63	F	22	3.5	13.1	28.3		3.3	3.4	0.5	
28	F	29	38.5	13.0			0.5				64	F	23	39.3	10.2	2.0			0.5		
29	M	22	31.5	11.0	7.5		0.5	1.5			65	M	21	45.0	5.5				1.5		
30	F	27	17.8	8.0	10.0	15.0		1.2			66	F	22	8.8	9.0	33.2		0.5	0.5		
31	M	20	48.0	3.5				0.5			67	F	21	7.8	10.5	13.7	18.5	0.5		1.0	
32	F	24	52.0								68	F	25	20.0	25.0	3.5		1.0	2.0	0.5	
33	F	25	52.0								69	M	24	16.8	22.2	8.5		2.5	2.0		
34	M	21	6.3	10.1	9.5	25.2	0.9				70	F	24	24.5	5.0	4.5	13.0	2.1	2.4	0.5	
35	F	23	51.0					1.0			71	F	20	35.0	3.5	13.5					
36	M	23	19.0	17.0	11.0		3.5	1.5													

Table B2
Mean and standard deviation (min) of sleep staged epochs with total time ≥ 5 min.

	Long (≥1 min)			
	W	N1	N2	N3
Number of subjects	65	45	35	16
Mean ± SD	31.3 ± 15.6	13.0 ± 7.8	15.1 ± 6.7	17.9 ± 7.2

References

Allen, P.J., Polizzi, G., Krakow, K., Fish, D.R., Lemieux, L., 1998. Identification of EEG events in the MR scanner: the problem of pulse artifact and a method for its subtraction. NeuroImage 8, 229–239.

Altmann, A., Schroter, M.S., Spoormaker, V.I., Kiem, S.A., Jordan, D., Ilg, R., Bullmore, E.T., Greicius, M.D., Czisch, M., Samann, P.G., 2016. Validation of non-REM sleep stage decoding from resting state fMRI using linear support vector machines. NeuroImage 125, 544–555.

Anderson, K.N., Hatfield, C., Kipps, C., Hastings, M., Hodges, J.R., 2009. Disrupted sleep and circadian patterns in frontotemporal dementia. Eur. J Neurol. 16, 317–323.

Bargmann, C.I., Marder, E., 2013. From the connectome to brain function. Nat. Method. 10, 483–490.

Bates, D., Machler, M., Bolker, B.M., Walker, S.C., 2015. Fitting linear mixed-effects models using lme4. J. Stat. Soft 67, 1–48.

Bates, E., Reilly, J., Wulfeck, B., Dronkers, N., Opie, M., Fenson, J., Kriz, S., Jeffries, R., Miller, L., Herbst, K., 2001. Differential effects of unilateral lesions on language production in children and adults. Brain Lang. 79, 223–265.

Biswal, B., Yetkin, F.Z., Haughton, V.M., Hyde, J.S., 1995. Functional connectivity in the motor cortex of resting human brain using echo-planar MRI. Magn. Reson. Med. 34, 537–541.

Boly, M., Perlbarg, V., Marrelec, G., Schabus, M., Laureys, S., Doyon, J., Pelegrini-Issac, M., Maquet, P., Benali, H., 2012. Hierarchical clustering of brain activity during human nonrapid eye movement sleep. Proceedings Natl. Acad. Sci. U S A.

Born, A.P., Law, I., Lund, T.E., Rostrup, E., Hanson, L.G., Wildschiodtz, G., Lou, H.C., Paulson, O.B., 2002. Cortical deactivation induced by visual stimulation in human slow-wave sleep. Neuroimage 17, 1325–1335.

Boyle, P.J., Scott, J.C., Krentz, A.J., Nagy, R.J., Comstock, E., Hoffman, C., 1994. Diminished brain glucose metabolism is a significant determinant for falling rates of systemic glucose utilization during sleep in normal humans. J. Clin. Invest. 93, 529–535.

Braun, A.R., Balkin, T.J., Wesenten, N.J., Carson, R.E., Varga, M., Baldwin, P., Selbie, S., Belenky, G., Herscovitch, P., 1997. Regional cerebral blood flow throughout the sleep-wake cycle. An H2(15)O PET study. Brain 120 (Pt 7), 1173–1197.

Broca, P., 1861. Perte de la parole: ramollissement chronique et destruction partielle du lobe anterieur gauche du cerveau. Bull. De. La. Soc. D.'Anthr., 1re Ser. 2, 235–238.

Buchsbaum, M.S., Gillin, J.C., Wu, J., Hazlett, E., Sicotte, N., Dupont, R.M., Bunney, W.E., Jr, 1989. Regional cerebral glucose metabolic rate in human sleep assessed by positron emission tomography. Life Sci. 45, 1349–1356.

Cai, Q., Van der Haegen, L., Brysbaert, M., 2013. Complementary hemispheric specialization for language production and visuospatial attention. Proc. Natl. Acad. Sci. U S A 110, E322–E330.

Chaudhuri, K.R., Healy, D.G., Schapira, A.H.V., 2006. Non-motor symptoms of Parkinson's disease: diagnosis and management. Lancet Neurol. 5, 235–245.

Chow, H.M., Horovitz, S.G., Carr, W.S., Picchioni, D., Coddington, N., Fukunaga, M., Xu, Y., Balkin, T.J., Duyn, J.H., Braun, A.R., 2013. Rhythmic alternating patterns of brain activity distinguish rapid eye movement sleep from other states of consciousness. Proc. Natl. Acad. Sci. U S A 110, 10300–10305.

Damasio, H., Tranel, D., Grabowski, T., Adolphs, R., Damasio, A., 2004. Neural systems behind word and concept retrieval. Cognition 92, 179–229.

Dang-Vu, T.T., Schabus, M., Desseilles, M., Albouy, G., Boly, M., Darsaud, A., Gais, S., Rauchs, G., Sterpenich, V., Vandewalle, G., Carrier, J., Moonen, G., Balteau, E., Degueldre, C., Luxen, A., Phillips, C., Maquet, P., 2008. Spontaneous neural activity during human slow wave sleep. Proc. Natl. Acad. Sci. USA 105, 15160–15165.

Davis, B., Tagliazucchi, E., Jovicich, J., Laufs, H., Hasson, U., 2016. Progression to deep sleep is characterized by changes to BOLD dynamics in sensory cortices. NeuroImage 130, 293–305.

Deuker, L., Olligs, J., Fell, J., Kranz, T.A., Mormann, F., Montag, C., Reuter, M., Elger, C.E., Axmacher, N., 2013. Memory consolidation by replay of stimulus-specific neural activity. J. Neurosci. 33, 19373–19383.

Diekelmann, S., Born, J., 2010. The memory function of sleep. Nat. Rev. Neurosci. 11, 114–126.

Forman, S.D., Cohen, J.D., Fitzgerald, M., Eddy, W.F., Mintun, M.A., Noll, D.C., 1995. Improved assessment of significant activation in functional magnetic resonance imaging (fMRI): use of a cluster-size threshold. Magn. Reson. Med. 33, 636–647.

Foulkes, D., Scmidt, M., 1983. Temporal sequence and unit composition in dream reports from different stages of sleep. SLEEP 6, 265–280.

Fox, M.D., Zhang, D., Snyder, A.Z., Raichle, M.E., 2009. The global signal and observed anticorrelated resting state brain networks. J. Neurophysiol. 101, 3270–3283.

Fransson, P., Skiold, B., Engstrom, M., Hallberg, B., Mosskin, M., Aden, U., Lagercrantz, H., Blennow, M., 2009. Spontaneous brain activity in the newborn brain during natural sleep–an fMRI study in infants born at full term. Pediatr. Res. 66, 301–305.

Friston, K., 2012. Ten ironic rules for non-statistical reviewers. NeuroImage 61, 1300–1310.

Friston, K.J., Holmes, A.P., Poline, J.B., Grasby, P.J., Williams, S.C., Frackowiak, R.S., Turner, R., 1995. Analysis of fMRI time-series revisited. Neuroimage 2, 43–53.

Friston, K.J., Williams, S., Howard, R., Frackowiak, R.S., Turner, R., 1996. Movement-related effects in fMRI time-series. Magn. Reson. Med. 35, 346–355.

Fukunaga, M., Horovitz, S.G., van Gelderen, P., de Zwart, J.A., Jansma, J.M., Ikonomidou, V.N., Chu, R., Deckers, R.H., Leopold, D.A., Duyn, J.H., 2006. Large-amplitude, spatially correlated fluctuations in BOLD fMRI signals during extended rest and early sleep stages. Magn. Reson. Imaging 24, 979–992.

Gazzaniga, M.S., 1983. Right hemisphere language following brain bisection: a 20-year perspective. Am. Psychol. 38, 525–537.

Gazzaniga, M.S., 2000. Cerebral specialization and interhemispheric communication: does the corpus callosum enable the human condition? Brain 123 (Pt 7), 1293–1326.

Gazzaniga, M.S., Bogen, J.E., Sperry, R.W., 1962. Some functional effects of sectioning the cerebral commissures in man. Proc. Natl. Acad. Sci. U S A 48, 1765–1769.

Gee, D.G., Biswal, B.B., Kelly, C., Stark, D.E., Margulies, D.S., Shehzad, Z., Uddin, L.Q., Klein, D.F., Banich, M.T., Castellanos, F.X., Milham, M.P., 2011. Low frequency fluctuations reveal integrated and segregated processing among the cerebral hemispheres. Neuroimage 54, 517–527.

Gold, C.A., Budson, A.E., 2008. Memory loss in Alzheimer's disease: implications for development therapeutics. Expert Rev. Neurother., 1879–1891.

Hahamy, A., Calhoun, V., Pearlson, G., Harel, M., Stern, N., Attar, F., Malach, R., Solomon, R., 2014. Save the global: global signal connectivity as a tool for studying clinical populations with functional magnetic resonance imaging. Brain Connect 4, 395–403.

Heilman, K.M., Abell, T.V.D., 1980. Right hemisphere dominance for attention. Neurology 30, 327–330.

Hobson, J.A., 2005. Sleep is of the brain, by the brain and for the brain. Nature 437, 1254–1256.

Hofle, N., Paus, T., Reutens, D., Fiset, P., Gotman, J., Evans, A.C., Jones, B.E., 1997. Regional cerebral blood flow changes as a function of delta and spindle activity during slow wave sleep in humans. J. Neurosci. 17, 4800–4808.

Horikawa, T., Tamaki, M., Miyawaki, Y., Kamitani, Y., 2013. Neural decoding of visual imagery durying sleep. Science 340, 639–642.

Horovitz, S.G., Braun, A.R., Carr, W.S., Picchioni, D., Balkin, T.J., Fukunaga, M., Duyn, J.H., 2009. Decoupling of the brain's default mode network during deep sleep. Proc. Natl. Acad. Sci. U S A 106, 11376–11381.

Horovitz, S.G., Fukunaga, M., de Zwart, J.A., van Gelderen, P., Fulton, S.C., Balkin, T.J., Duyn, J.H., 2008. Low frequency BOLD fluctuations during resting wakefulness and ligt sleep: a simultaneous EEG-fMRI study. Hum. Brain Mapp. 29, 671–682.

Hougaard, A., Jensen, B.H., Amin, F.M., Rostrup, E., Hoffman, M.B., Ashina, M., 2015. Cerebral asymmetry of fMRI-BOLD responses to visual stimulation. PLoS ONE 10, e0126477.

Ju, Y.-E.S., Lucey, B., Holtzman, D.M., 2014. Sleep and Alzheimer disease pathology - a bidirectional relationship. Nat. Rev. Neurol. 10, 115–119.

Kajimura, N., Uchiyama, M., Takayama, Y., Uchida, S., Uema, T., Kato, M., Sekimoto, M., Watanabe, T., Nakajima, T., Horikoshi, S., Ogawa, K., Nishikawa, M., Hiroki, M., Kudo, Y., Matsuda, H., Okawa, M., Takahashi, K., 1999. Activity of midbrain reticular formation and neocortex during the progression of human non-rapid eye movement sleep. J. Neurosci. 19, 10065–10073.

Kaufmann, C., Wehrle, R., Wetter, T.C., Holsboer, F., Auer, D.P., Pollmacher, T., Czisch, M., 2006. Brain activation and hypothalamic functional connectivity during human non-rapid eye movement sleep: an EEG/fMRI study. Brain 129, 655–667.

Kjaer, T.W., Law, I., Wiltschiotz, G., Paulson, O.B., Madsen, P.L., 2002. Regional cerebral blood flow during light sleep - a $H^{152}O$-PET study. J. Sleep. Res. 11, 201–207.

Kristensen, L.B., Wang, L., Petersson, K.M., Hagoort, P., 2013. The interface between language and attention: prosodic focus marking recruits a general attention network in spoken language comprehension. Cereb. Cortex 23, 1836–1848.

Laufs, H., Walker, M.C., Lund, T.E., 2007. Letter to the editor: 'brain activation and hypothalamic functional connectivity during human non-rapid eye movement sleep: an EEG/fMRI study' - its limitations and an alternative approachBrain 130, e75.

LeDoux, J.E., Wilson, D.H., Gazzaniga, M.S., 1977. Manipulo-spatial aspects of cerebral lateralization: clues to the origin of lateralization. Neuropsychologia 15, 743–750.

Levy, J., 1969. Possible basis for the evolution of lateral specialization of the human brain. Nature 224, 614–615.

Liu, H., Stufflebeam, S.M., Sepulcre, J., Hedden, T., Buckner, R.L., 2009. Evidence from intrinsic activity that asymmetry of the human brain is controlled by multiple factors. Proc. Natl. Acad. Sci. USA 106, 20499–20503.

Lowe, M.J., Mock, B.J., Sorenson, J.A., 1998. Functional connectivity in single and multislice echoplanar imaging using resting-state fluctuations. Neuroimage 7,

119–132.
Madsen, P.L., Schmidt, J.F., Wildschiodtz, G., Friberg, L., Holm, S., Vorstrup, S., Lassen, N.A., 1991. Cerebral O2 metabolism and cerebral blood flow in humans during deep and rapid-eye-movement sleep. J Appl. Physiol. 70, 2597–2601.
Mapstone, M., Weintraub, S., Nowinski, C., Kaptanoglu, G., Gitelman, D.R., Mesulam, M.M., 2003. Cerebral hemispheric specialization for spatial attention: spatial distribution of search-related eye fixations in the absence of neglect. Neuropsychologia 41, 1396–1409.
Maquet, P., Degueldre, C., Delfiore, G., Aerts, J., Peters, J.M., Luxen, A., Franck, G., 1997. Functional neuroanatomy of human slow wave sleep. J Neurosci. 17, 2807–2812.
McAvoy, M., Mitra, A., Coalson, R.S., d'Avossa, G., Keidel, J.K., Petersen, S.E., Raichle, M.E., 2015. Unmasking language lateralization in human brain intrinsic activity. Cereb. Cortex, 1–14.
McAvoy, M.P., Ollinger, J.M., Buckner, R.L., 2001. Cluster size thresholds for assessment of significant activation in fMRI. Neuroimage 13, S198.
Mitra, A., Snyder, A.Z., Tagliazucchi, E., Laufs, H., Raichle, M.E., 2015. Propagated infra-slow intrinsic brain activity reorganizes across wake and slow wave sleep. eLife 4, 1–19.
Nofzinger, E.A., Buysse, D.J., Miewald, J.M., Meltzer, C.C., Price, J.C., Sembrat, R.C., Ombao, H., Reynolds, C.F., 3rd, Monk, T.H., Hall, M., Kupfer, D.J., Moore, R.Y., 2002. Human regional cerebral glucose metabolism during non-rapid eye movement sleep in relation to waking. Brain 125, 1105–1115.
Ohayon, M.M., Carskadon, M.A., Guilleminault, C., Vitiello, M.V., 2004. Meta-analysis of quantitative sleep parameters from childhood to old age in healthy individuals: developing normative sleep values across the human lifespan. Sleep 27, 1255–1273.
Ojemann, J.G., Akbudak, E., Snyder, A.Z., McKinstry, R.C., Raichle, M.E., Conturo, T.E., 1997. Anatomic localization and quantitative analysis of gradient refocused echo-planar fMRI susceptibility artifacts. Neuroimage 6, 156–167.
Pardo, J.V., Fox, P.T., Raichle, M.E., 1991. Localization of a human system for sustained attention by positron emission tomography. Nature 349, 61–64.
Petit, L., Zago, L., Mellet, E., Jobard, G., Crivello, F., Joloit, M., Mazoyer, B., Tzourio-Mazoyer, N., 2015. Strong rightward lateralization of the dorsal attentional network in left-handers with right sighting-eye: an evolutionary advantage. Hum. Brain Mapp. 36, 1151–1164.
Power, J.D., Barnes, K.A., Snyder, A.Z., Schlaggar, B.L., Petersen, S.E., 2012. Spurious but systematic correlations in functional connectivity MRI networks arise from subject motion. Neuroimage 59, 2142–2154.
Power, J.D., Mitra, A., Laumann, T.O., Snyder, A.Z., Schlaggar, B.L., Petersen, S.E., 2014. Methods to detect, characterize, and remove motion artifact in resting state fMRI. Neuroimage 84, 320–341.
Price, C.J., 2010. The anatomy of language: a review of 100 fMRI studies published in 2009. Ann. N Y Acad. Sci. 1191, 62–88.
Price, C.J., 2012. A review and synthesis of the first 20 years of PET and fMRI studies of heard speech, spoken language and reading. Neuroimage 62, 816–847.
Rabuffetti, M., Farina, E., Alberoni, M., Pellegatta, D., Ildebrando, A., Affanni, P., Forni, M., Ferrarin, M., 2012. Spatio-temporal features of visual exploration in unilaterally brain-damaged subjects with or without neglect: results from a touchscreen test. PLoS ONE 7, e31511.
Rowland, D.J., Garbow, J.R., Laforest, R., Snyder, A.Z., 2005. Registration of [18F]FDG microPET and small-animal MRI. Nucl. Med. Biol. 32, 567–572.
Scholvinck, M.L., Maier, A., Ye, F.Q., Duyn, J.H., Leopold, D.A., 2010. Neural basis of global resting-state fMRI activity. Proc. Natl. Acad. Sci. U S A 107, 10238–10243.
Shmueli, K., van Gelderen, P., de Zwart, J.A., Horovitz, S.G., Fukunaga, M., Jansma, J.M., Duyn, J.H., 2007. Low-frequency fluctuations in the cardiac rate as a source of variance in the resting-state fMRI BOLD signal. Neuroimage 38, 306–320.
Shulman, G.L., Pope, D.L., Astafiev, S.V., McAvoy, M.P., Snyder, A.Z., Corbetta, M., 2010. Right hemisphere dominance during spatial selective attention and target detection occurs outside the dorsal frontoparietal network. J Neurosci. 30, 3640–3651.
Silber, M.H., Ancoli-Israel, S., Bonnet, M.H., Chokroverty, S., Grigg-Damberger, M.M., Hirshkowitz, M., Kapen, S., Keenan, S.A., Kryger, M.H., Penzel, T., Pressman, M.R., Iber, C., 2007. The visual scoring of sleep in adults. J. Clin. Sleep. Med 3, 121–131.
Spoormaker, V.I., Schroter, M.S., Gleiser, P.M., Andrade, K.C., Dresler, M., Wehrle, R., Samann, P.G., Czisch, M., 2010. Development of a large-scale functional brain network during human non-rapid eye movement sleep. J. Neurosci. 30, 11379–11387.
Stelzmann, R.A., Schnitzlein, H.N., Murtagh, F.R., 1995. An English translation of Alzheimer's 1907 paper, Uber eine eigenartige Erkankung der Hirnrinde. Clin. Anat., 429–431.
Tagliazucchi, E., Behrens, M., Laufs, H., 2013a. Sleep neuroimaging and models of consciousness. Front Psychol. 4, 1–9.
Tagliazucchi, E., Crossley, N., Bullmore, E.T., Laufs, H., 2015. Deep sleep divides the cortex into opposite modes of anatomical-functional coupling. Brain Struct. Funct., 1–14.
Tagliazucchi, E., Laufs, H., 2014. Decoding wakefulness levels from typical fMRI resting-state data reveals reliable drifts between wakefulness and sleep. Neuron 82, 695–708.
Tagliazucchi, E., von Wegner, F., Morzelewski, A., Borisov, S., Jahnke, K., Laufs, H., 2012. Automatic sleep staging using fMRI functional connectivity data. Neuroimage 63, 63–72.
Tagliazucchi, E., von Wenger, F., Morzelewski, A., Brodbeck, V., Jahnke, K., Laufs, H., 2013b. Breakdown of long-range temporal dependence in default mode and attention networks during deep sleep. PNAS 110, 15419–15424.
Talairach, J., Tournoux, P., 1988. Co-Planar Stereotaxic Atlas of the Human Brain. Thieme Medical Publishers, Inc., New York.
Taler, V., Phillips, V.T., 2008. Language performance in Alzheimer's disease and mild cognitive impairment: a comparative review. J. Clin. Exp. Neuropsychol. 30, 501–556.
Tamaki, M., Bang, J.W., Watanabe, T., Sasaki, Y., 2014. The first-night effect suppresses the strength of slow-wave activity originating in the visual areas during sleep. Vis. Res. 99, 154–161.
Tamaki, M., Bang, J.W., Watanabe, T., Sasaki, Y., 2016. Night watch in one brain hemisphere during sleep associated with the first-night effect in humans. Curr. Biol. 26, 1190–1194.
Tucker, D.M., Williamson, P.A., 1984. Asymmetric neural control systems in human self-regulation. Psychol. Rev. 91, 185–215.
Uehara, T., Yamasaki, T., Okamoto, T., Koike, T., Kan, S., Miyauchi, S., Kira, J.I., Tobimatsu, S., 2013. Efficiency of a "Small-World" Brain Network Depends on Consciousness Level: A Resting-State fMRI Study. Cereb Cortex.
Walker, M.P., Stickgold, R., 2006. Sleep, memory, and plasticity. Annu Rev. Psychol. 57, 139–166.
Wang, D., Buckner, R.L., Liiu, H., 2013. Cerebellar asymmetry and its relation to cerebral asymmetry estimated by intrinsic functional connectivity. J Neurophysiol. 109, 46–57.
Wang, D., Buckner, R.L., Liu, H., 2014. Functional specialization in the human brain estimated by intrinsic hemispheric interaction. J Neurosci. 34, 12341–12352.
Weintraub, S., Wicklund, A.H., Salmon, D.P., 2012. The Neuropsychological profile of Alzheimer disease. Cold Spring Harb. Perspect. Med 2, a006171.
Weissenbacher, A., Kasess, C., Gerstl, F., Lazenberger, R., Moser, E., Windischberger, C., 2009. Correlations and anticorrelations in resting-state functional connectivity MRI: a quantitative comparison of preprocessing strategies. Neuroimage 47, 1408–1416.
Wernicke, C., 1874. . Der Aphasische Symptomencomplex. Cohn and Weigert, Breslau.
Wise, R.G., Ide, K., Poulin, M.J., Tracey, I., 2004. Resting fluctuations in arterial carbon dioxide induce significant low frequency variations in BOLD signal. Neuroimage 21, 1652–1664.
Wong, C.W., Olafsson, V., Tal, O., Liu, T.T., 2013. The amplitude of the resting-state fMRI global signal is related to EEG vigilance measures. Neuroimage 83, 983–990.
Xie, L., Kang, H., Q., X., Chen, M.J., Liao, Y., hiyagarajan, M., O'Donnell, J., Christensen, D.J., Nicholson, C., Iliff, J.J., Takano, T., Deane, R., Nedergaard, M., 2013. Sleep drives metabolite clearance from the adult brain. Science 342, 373–377.
Yeo, B.T.T., Tandi, J., Chee, W.L.C., 2015. Functional connectivity during rested wakefulness predicts vulnerability to sleep deprivation. NeuroImage 111, 147–158.
Zeng, L.-L., Wang, D., Fox, M.D., Sabuncu, M., Hu, D., Ge, M., Buckner, R.L., Liu, H., 2014. Neurobiological basis of head motion in brain imaging. Proc. Natl. Acad. Sci. U S A 111, 6058–6062.